Inorganic Chemistry

Article

pubs.acs.org/IC

The Incommensurately Modulated Structures of the Perovskites $NaCeMnWO_6$ and $NaPrMnWO_6$

Susana García-Martín,[†] Graham King,*[,‡] Gwilherm Nénert,[§] C. Ritter,[§] and Patrick M. Woodward[⊥]

[†]Departamento de Química Inorgánica, Facultad de Ciencias Químicas, Universidad Complutense, Madrid 28040, Spain

[‡]Lujan Neutron Scattering Center, Los Alamos National Laboratory, MS H805, Los Alamos, New Mexico, 87545, United States

[§]Institut Laue-Langevin, 6 rue Jules Horowitz, 38042 Grenoble Cedex 9, France

[⊥]Department of Chemistry, The Ohio State University, 100 West 18th Avenue, Columbus, Ohio 43210-1185, United States

Supporting Information

ABSTRACT: The structures of the doubly ordered perovskites $NaCeMnWO_6$ and $NaPrMnWO_6$, with rock salt ordering of the Mn^{2+} and W^{6+} *B*-site cations and layered ordering of the Na^+ and (Ce^{3+}/Pr^{3+}) *A*-site cations, have been studied by transmission electron microscopy, electron diffraction, neutron and synchrotron X-ray powder diffraction. Both compounds possess incommensurately modulated crystal structures. In $NaCeMnWO_6$ the modulation vector (with reference to the ideal ABX_3 perovskite subcell) is $q \approx 0.067a^*$ (~58.7 Å) and in $NaPrMnWO_6$ $q \approx 0.046a^*$ (~85.3 Å). In both compounds the superstructures are primarily the two-dimensional chessboard type, although some crystals of $NaCeMnWO_6$ were found with one-dimensional stripes. In some crystals of $NaPrMnWO_6$ there is a coexistence of chessboards and stripes. Modeling of neutron diffraction data shows that octahedral tilting plays an important role in the structural modulation.

INTRODUCTION

Oxides with perovskite related structures that contain both transition metal and lanthanide cations show a great variety of optical, magnetic, and electric properties. The perovskite structure (ABX_3) can often accommodate the substitution of multiple cations onto either the *A* or *B*-sites to form quaternary ($A_2B_{2-x}B'_xX_6$ or $A_{2-x}A'_xB_2X_6$) or quintinary ($A_{2-x}A'_xB_{2-y}B'_yX_6$) compounds, which allows for great flexibility in materials design and the tuning of crystal structures and properties.

When multiple cations are substituted onto either the *A* or *B*-sites, these cations may be either randomly distributed or adopt an ordered configuration.[1] Rock salt ordering of two *B*-site cations present in a 1:1 ratio is commonly observed when there is sufficient difference in size and charge between them. Ordering of *A*-site cations is much less common, but when it does occur the ordering is usually in a layered fashion. There have been several recent studies on perovskites with nominal stoichiometry $AA'BB'O_6$ which show the rather unusual combination of both rock salt ordering of *B*/*B*′ and layered ordering of *A*/*A*′.[1−5] In addition to this cation ordering, some $AA'BB'O_6$ phases also spontaneously form large superstructures because of modulations of the crystal structures, suggesting new systems to search for self-assembled nanostructures.[6−8]

The superstructures that are found in doubly ordered $AA'BB'O_6$ perovskites consist of both a compositional modulation of the crystal structure related to the *A*-site cations and a twinning of the octahedral tilt system. Transmission electron microscopy (TEM), scanning transmission electron microscopy (STEM), and electron energy loss spectroscopy (EELS) measurements have shown that these materials are composed of two compositionally distinct domains.[6,7] In all compounds studied so far *A* is an alkali cation (Na^+ or K^+) and *A*′ is a trivalent lanthanide cation (Ln^{3+}). One of the compositional domains is thought to have an *A*:*A*′ ratio close to 1:1 where the *A* and *A*′ cations are simply ordered into layers. In the other domain the Ln^{3+} layer remains intact, but there is a significant deficiency of Na^+ or K^+ within the alkali layer. One third of the alkali vacancies are thought to be occupied by Ln^{3+} cations to retain charge balance, giving this domain a composition of $A_{1-3x}A'_{1+x}BB'O_6$.

Neutron powder diffraction (NPD) measurements have also shown that a twinning of the octahedral tilt system accompanies these compositional modulations and occurs with the same periodicity.[7,9] Interestingly, in all of the compounds studied so far that show this type of modulation the underlying tilt system can be described as $a^-a^-c^0$ in Glazer notation.[10,11] Octahedral tilt twinning occurs when the out-of-phase tilting is interrupted by an in-phase tilt. These twin boundaries are thought to occur to alleviate the strain that arises from the crystallographic mismatch between the different compositional domains. It is important to mention that neither the compositional modulation nor the twinning of the octahedral tilt system is evident in the X-ray diffraction (XRD) patterns of these materials.

To date, the superstructures of three $AA'BB'O_6$ perovskites have been reported in detail. $NaLaMgWO_6$ has a one-dimensional (1-D) superstructure consisting of compositionally

Received: September 22, 2011
Published: March 2, 2012

   dx.doi.org/10.1021/ic202071n | *Inorg. Chem.* 2012, 51, 4007−4014

distinct stripes each $6a_p$ wide (a_p is the unit cell dimension of the ideal ABX_3 subcell, ~3.95 Å) giving a supercell with dimensions of $12a_p \times 2a_p \times 2a_p$.[6] Neutron powder diffraction has been used to show there is a twinning of the octahedral tilt system, which also occurs in one dimension.[9] $KLaMnWO_6$ forms a two-dimensional (2-D) chessboard-type superlattice which has a periodicity of $10a_p \times 10a_p \times 2a_p$.[7] In this compound the tilt twinning is also 2-D. A similar chessboard-type superstructure has also been recently observed in $NaNdMgWO_6$, except in this case the supercell dimensions are $14a_p \times 14a_p \times 2a_p$.[8]

One notable feature of $KLaMnWO_6$ is that its XRD pattern can be indexed using a tetragonal unit cell. The supercell reflections due to the larger unit cell size are too weak in the XRD patterns to be seen and so the compound appears to have a simple $\sqrt{2}a_p \times \sqrt{2}a_p \times 2a_p$ tetragonal unit cell even according to synchrotron XRD. In doubly ordered $AA'BB'O_6$ perovskites the aristotype structure (no octahedral tilting) has tetragonal symmetry because of the layered ordering of the *A*-site cations.[2] Most of the common octahedral tilting patterns lead to monoclinic symmetry; therefore, tetragonal lattice parameters could be taken as an indication that octahedral tilting is absent. Modeling of the octahedral tilt twinning in $KLaMnWO_6$ has shown that the symmetry of the supercell (ignoring the compositional variation) is indeed tetragonal.

Another recent study has used XRD to look at the progression of the unit cell parameters in two series of $NaLnMnWO_6$ and $NaLnMgWO_6$ compounds as *Ln* is varied.[4] The general finding was that for larger *Ln* (Ce and Pr, but not La) metrically tetragonal lattice parameters are observed, and for smaller *Ln* (Nd−Ho) monoclinic unit cells result. The monoclinic compounds most likely have polar $P2_1$ space group symmetry, which corresponds to $a^-a^-c^+$ octahedral tilting. For the $NaLnMnWO_6$ compounds with *Ln* = La, Nd, and Tb neutron diffraction has conclusively confirmed the symmetry is $P2_1$.[3] The additional in-phase tilt about the *c*-axis is incompatible with the formation of octahedral tilt twin boundaries. One puzzling aspect of these findings is that the compounds which appear to be tetragonal have tolerance factors which are far too small for these compounds to be stable without some form of octahedral tilting. Bond valence optimizations strongly predict $a^-a^-c^+$ as the most stable tilt system and suggest that the tetragonal aristotype structure should be highly unstable.[12,13] Based on these results and the results of our recent study of $KLaMnWO_6$, we have hypothesized that those compounds which appear to be tetragonal according to XRD in fact have $a^-a^-c^0$ octahedral tilting, which is twinned in both directions. The presence of tilt twinning would imply that these compounds are also compositionally modulated.

In this study we examine $NaCeMnWO_6$ and $NaPrMnWO_6$, which are the two compounds of the $NaLnMnWO6$ series which show tetragonal lattice parameters according to XRD analysis. Both compounds have small tolerance factors (τ = 0.926 and τ = 0.924 respectively), which strongly suggests that some form of octahedral tilting must be present. These compounds also show interesting magnetic phase transitions at low temperature.[4,5] Here we present a study of the crystal structures of $NaCeMnWO_6$ and $NaPrMnWO_6$ by means of selected area electron diffraction (SAED), high resolution transmission electron microscopy (HRTEM), neutron powder diffraction (NPD), and synchrotron X-ray powder diffraction (XRD). We show that the structures of these compounds are more complex than previously thought because of incommensurate modulations of their crystal structure.

EXPERIMENTAL SECTION

$NaCeMnWO_6$ and $NaPrMnWO_6$ were prepared by the ceramic method using as starting materials: Na_2CO_3 (Fisher, 99.9%), $MnWO_4$ (Alfa Aesar, 99.9%), CeO_2 (Acros, 99.9%), and Pr_6O_{11} (Alfa Aesar, 99.9%). CeO_2 and Pr_6O_{11} were heated to 900 °C for 6 h prior to use to remove any absorbed water or CO_2. A 2% excess of Na_2CO_3 was used to account for the high temperature volatility of sodium. Stoichiometric amounts of the reactants were ground and heated at 1000 °C for 8 h under the flow of forming gas (5% H_2, 95% N_2) to prevent the oxidation of Mn^{2+} to Mn^{3+}. After regrinding, the samples were annealed under the same conditions for an additional 24 h to thermodynamically stabilize the complex superstructure.

For TEM the samples were ground in *n*-butyl alcohol and ultrasonically dispersed. A few drops of the resulting suspension were deposited in a carbon coated grid. SAED and HRTEM studies were carried out with a JEM 3000F microscope operating at 300 kV (double tilt (±20°) (point resolution 1.7 Å), fitted with an ENFINA 1000 spectrometer and a JEOL annular dark field (ADF) detector.

Neutron powder diffraction data were collected on the high resolution diffractometer D1A at the Institut Laue-Langevin using a wavelength of 1.909 Å. The NPD pattern of the $NaCeMnWO_6$ sample was collected at 300 K and the NPD pattern of $NaPrMnWO_6$ was collected at 100 K. Synchrotron X-ray powder diffraction patterns were collected at the ESRF on the high-resolution powder diffractometer ID31 using a wavelength of 0.396 Å. The XRD pattern of the $NaCeMnWO_6$ sample was collected at 220 K, and the NPD pattern of $NaPrMnWO_6$ was collected at 255 K. Rietveld refinements were done using the GSAS/EXPGUI software package.[14,15]

RESULTS

Transmission Electron Microscopy. A complete study of the reciprocal lattices was performed by taking ED patterns by tilting different crystals of $NaCeMnWO_6$ and $NaPrMnWO_6$ along different zone axes. Both oxides show similar results. Figure 1 shows three representative SAED patterns along

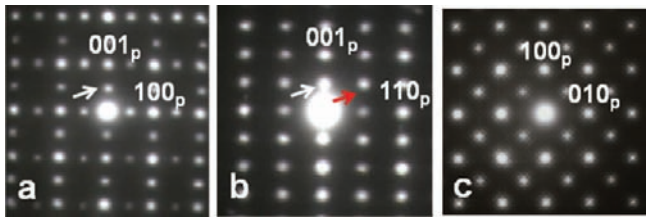

Figure 1. SAED patterns of a $NaCeMnWO_6$ crystal along the (a) $[010]_p$, (b) $[\bar{1}10]_p$, and (c) $[001]_p$ zone axes.

different zone axes of a crystal of $NaCeMnWO_6$. The patterns have been indexed according to the ideal cubic perovskite structure. In addition to the main Bragg reflections, there are strong superlattice reflections related to the *A*-site cation layered ordering, like $1/2\ (001)_p$ indicated by a white arrow in the patterns of Figure 1, and reflections related to rock salt-type ordering of the Mn and W ions (for instance the $1/2\ (111)_p$ reflection indicated by a red arrow in the pattern corresponding to the $[\bar{1}10]_p$ zone axis). Although it is not possible to uniquely identify the octahedral tilt system in complex perovskites with *A* and *B*-site cation ordering and twinning and domain formations, there are some weak reflections which could be related to the tilting system. The 1/2 (ooo) reflections could arise from out-of-phase tilting, but in this case most of their intensity is coming from *B*-site cation ordering. The 1/2(ooe)

dx.doi.org/10.1021/ic202071n | Inorg. Chem. 2012, 51, 4007−4014

$h \neq k$ reflections are usually associated to in-phase tilting of the octahedra around the c-axis[16] but cation ordering in combination with out-of-phase tilting of the octahedra leads to cation displacements, which could also account for the appearance of these reflections. The reciprocal lattice deduced from these reflections of the SAED patterns agree with an average $\sim\sqrt{2}a_p \times \sim\sqrt{2}a_p \times \sim 2a_p$ unit cell, which is confirmed by the HRTEM results. Moreover, satellite reflections appear around the $(100)_p$, $(010)_p$, and $(110)_p$ main Bragg reflections (Figure 1c) indicating modulation of the basic crystal structure along $[100]_p$, $[010]_p$ directions and satellites around 1/2 $(110)_p$ and equivalent positions, also along $[100]_p$, $[010]_p$, which were firstly ascribed to the formation of four antiphase domains due to twinning of the octahedral tilt system in perovskite-type niobates.[17−19]

The spacing between satellite reflections can be used to determine the periodicity of the modulation and the modulation vector.[20] In this case an incommensurate modulation is deduced; the modulation vector being $q = (1/N_{super})\ a^*$ with $q \approx 0.067\ a^*$, which corresponds to a periodicity of $\sim 14.9a_p$ ($\sim$58.7 Å) along both the $[100]_p$ and $[010]_p$ directions.

HRTEM images of these compounds also reveal a modulation of the crystal structure. Figure 2 shows several HRTEM images of a crystal of $NaCeMnWO_6$ along the $[001]_p$ zone axis and the corresponding SAED pattern or FFT pattern. The contrast differences indicate that the superstructure is arranged in the form of a chessboard pattern similar to $KLaMnWO_6$.[7] There are two different types of domains (dark and bright areas in the images of Figure 2a and c) arranged in a chessboard pattern. Four domains and the corresponding two perpendicular domain boundaries have been marked in red in Figure 2a. Therefore, there is modulation of the crystal structure along the $[100]_p$ and $[010]_p$ directions, in agreement with the satellite reflections appearing in the SAED pattern (see Figure 2b). The average size of the domains ($\sim 7.5a_p$) agrees with the periodicity deduced from the modulation vector in the ED pattern ($\sim 15a_p$). Incommensurate modulation is then confirmed by the HRTEM images, where it is clearly seen that the size of the domains is not uniform all over the entire crystal.

The modulation of the crystal structure may be caused by displacements of atoms, by variation in the occupancy of atom sites, or by both. If the modulation were due to small atomic displacements or small changes in atom scattering power because of occupancy variation, HRTEM images of thin crystals would be unlikely to show sufficient contrast to make the modulation apparent. However, the modulation may be visible in thick regions of the crystal because strong dynamical scattering increases the effects of small structural and chemical variation. Figure 2c shows an HRTEM image of a $NaCeMnWO_6$ crystal taken at Scherzer defocus on a thin region near the edge of the crystal. Strong contrast differences are clearly seen forming dark and bright domains arranged in a chessboard pattern. In Figure 2a, which was taken on a thick region of the crystal, contrast differences with $\sqrt{2}a_p$ periodicity most likely related to octahedral tilting can be seen. These contrast differences form slightly darker stripes which are superimposed with the contrast difference seen in Figure 2c, suggesting that there are two different structural features contributing to the modulation. Our previous work on $KLaMnWO_6$ and $NaLaMgWO_6$ has shown that these compounds both have a compositional modulation of the A-site cations which is coupled with a twinning of the octahedral tilt system. Because of the strong similarity between the underlying crystal structures of these two compounds and $NaCeMnWO_6$, as well as a strong similarity between the HRTEM images of $KLaMnWO_6$ and $NaCeMnWO_6$, these two

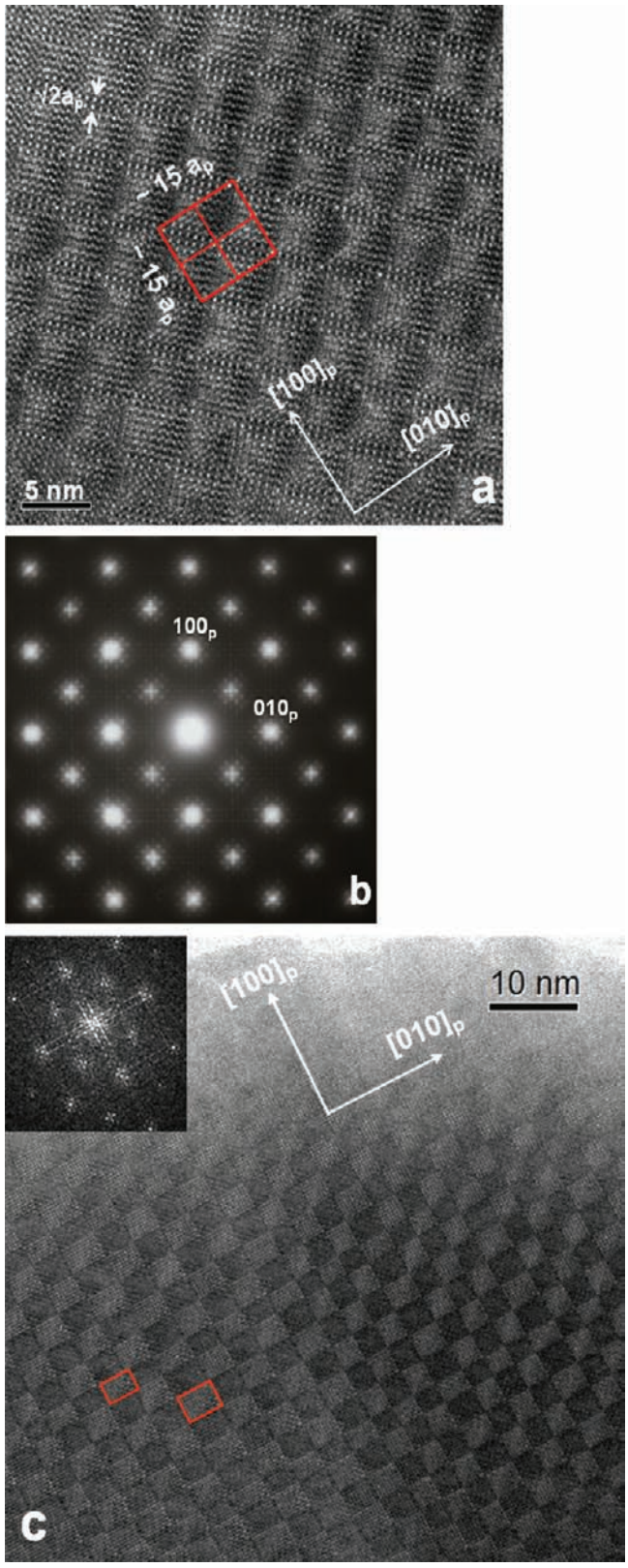

Figure 2. (a) HRTEM image, (b) SAED pattern, and (c) HRTEM image and the corresponding FFT of the $[001]_p$ zone axis of a $NaCeMnWO_6$ crystal.

dx.doi.org/10.1021/ic202071n | Inorg. Chem. 2012, 51, 4007−4014

structural features seem the most likely explanations for the observed HRTEM images. The weak contrast seen only in thick regions of the crystals can be attributed to a twinning of the octahedral tilt system since twinning only involves small displacements of weakly scattering oxygen atoms. The presence of octahedral tilt twinning has been confirmed by NPD studies, as discussed in the next section. The strong contrast differences which are seen even in thin regions of the crystals could be caused by a compositional modulation of the *A*-site cations since there is a large difference in scattering power between Na and Ce.

Another interesting feature of these samples is that most of the crystals contain large regions with different orientation that are separated by 90° boundaries. Figure 3a shows the HRTEM image of a crystal of $NaCeMnWO_6$ in the vicinity of the boundary separating two perpendicularly oriented regions. The FFT of this image is formed by superposition of the FFT of the two domains. This is the reason why $1/2(001)_p$ reflections appear along both $[001]_p$ and $[100]_p$ in the ED patterns (see Figure 1a and FFT in Figure 3a). Figure 3b shows the HRTEM of only one region of the crystal. In addition to the $\sim 2a_p$ periodicity, contrast differences related to the modulation of the crystal structure (tilt-twin boundaries) are seen. This orientation of the crystal confirms that the modulation of the structure occurs only along two directions ($[100]_p$ and $[010]_p$) and therefore, the superlattice structure keeps the $\sim 2a_p$ periodicity of the average structure (because of layered ordering of the A-cations) along the $[001]_p$ direction, like in $KLaMnWO_6$.[7]

Similar results are obtained for the $NaPrMnWO_6$ compound. The HRTEM images of this material also show an incommensurate modulation of the crystal structure forming a chessboard-type pattern (see Supporting Information). In the case of the Pr oxide, the modulation vector calculated in several crystals is $q \approx 0.046a^*$. This corresponds to an average periodicity of $N_{super} \sim 21.7a_p$, or about 85.3 Å. The HRTEM images of $NaPrMnWO_6$ show that the modulation vector in these crystals shows more variability than for the Ce analogue.

It is worth mentioning that in the $NaCeMnWO_6$ sample, we have found a few crystals in which the superstructure forms a stripe-pattern, similar to the modulation observed in $NaLaMgWO_6$.[5] Even more interesting is the fact that some crystals in the $NaPrMnWO_6$ sample have been found in which both types of patterns (stripes and chessboard) coexist in the same crystal. Figure 4 shows the HRTEM, SAED pattern, and FFT along the $[001]_p$ zone axis of one such crystal. In the HRTEM, twinning of the tilting system is highlighted and some domain boundaries have been indicated with red lines. Irregular nanopatterning has also previously been found in crystals of $0.85[(Nd_{1/2}Li_{1/2})TiO_3]-0.15[NdMO_3]$ with M = Al, Cr, Mn.[21]

Neutron Powder Diffraction. Neutron diffraction is the ideal method to study octahedral tilt twinning in $AA'BB'O_6$ perovskites because of its high sensitivity to oxygen positions. The NPD patterns of both $NaCeMnWO_6$ and $NaPrMnWO_6$ show many supercell reflections that cannot be indexed with any unit cell that only takes into account cation ordering and simple combinations of in-phase and out-of-phase octahedral tilting. The additional reflections appear as satellite peaks around several of the peaks of the $\sqrt{2}a_p \times \sqrt{2}a_p \times 2a_p$ tetragonal subcell, indicating that a large superstructure is present (Figure 5). Since these peaks were not observed in the previous XRD study,[4] the superstructure can be assumed to be due to oxygen atom positions. Considering our previous findings on $NaLaMgWO_6$ and $KLaMnWO_6$, a twinning of the octahedral tilt system seems the most likely explanation.

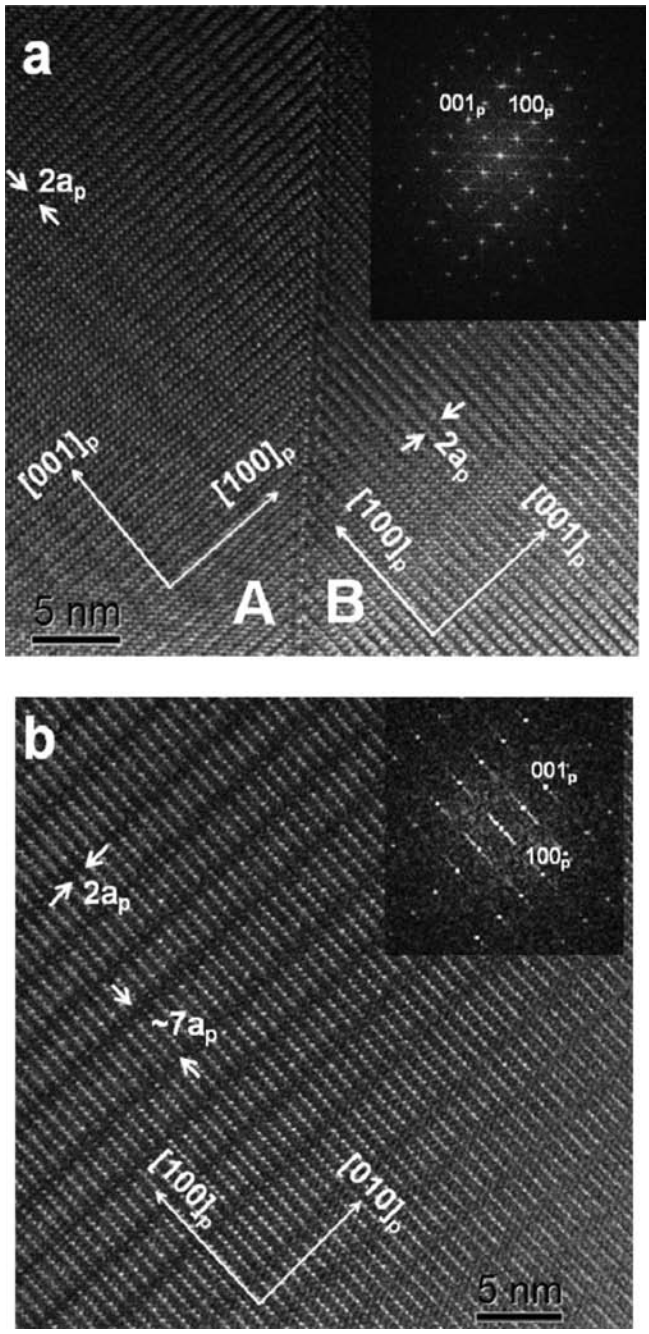

Figure 3. (a) HRTEM and FFT of two domains (A and B) of the $[001]_p$ zone axis perpendicularly oriented of a $NaCeMnWO_6$ crystal. (b) HRTEM and FFT of the domain B in panel a.

Because the supercells that result from octahedral tilt twinning contain a very large number of atoms, standard Rietveld refinements are not possible. In previous studies of related systems the construction of large model unit cells, which account for the superlattice formation due to periodical twinning of the tilting system (octahedral tilt angle was fixed and compositional modulation was not taken into account) and *B*-site cation displacements from the center of the octahedra have been used with success to model the positions and intensities of the satellite reflections in the NPD patterns.[7,9,22] We have attempted to do the same type of modeling with

dx.doi.org/10.1021/ic202071n | Inorg. Chem. 2012, 51, 4007–4014

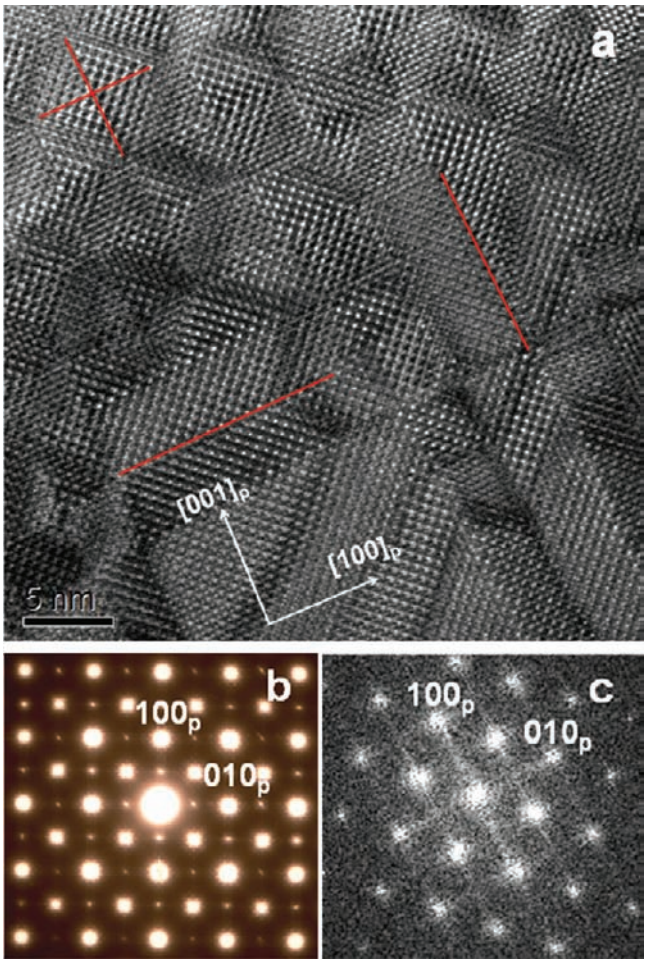

Figure 4. (a) HRTEM image, (b) SAED pattern, and (c) FFT of the $[001]_p$ zone axis of a $NaPrMnWO_6$ crystal.

$NaCeMnWO_6$ and $NaPrMnWO_6$, but the incommensurate nature of the modulation has prevented us from obtaining any good fits to the NPD patterns. In an attempt to model the NPD pattern of $NaCeMnWO_6$, supercells with $a^-a^-c^0$ tilting which have an octahedral tilt twin boundary every $7a_p$ along the a and b directions (giving a $14a_p \times 14a_p \times 2a_p$ unit cell) or every $8a_p$ (giving a $16a_p \times 16a_p \times 2a_p$ unit cell) were constructed and fitted against the experimental NPD pattern. Figure 6 shows a model of the unit cell formed by four domains separated by 2D twin boundaries giving a $14a_p \times 14a_p \times 2a_p$ periodicity. Neither model was able to provide a precise fit to the positions of the satellite peaks. With the $14a_p \times 14a_p \times 2a_p$ model the calculated satellite peaks were slightly too far from the subcell peaks, and for the $16a_p \times 16a_p \times 2a_p$ model the calculated satellite peaks were slightly too close to the subcell peaks. The best fit to the intensities of the peaks was realized with a model that had an octahedral tilt angle of 10°. This result is consistent with the ED results which show incommensurate modulation with an average periodicity to be between $14a_p$ and $16a_p$ and with the HRTEM results, which show different sizes of the domains forming the chessboard pattern. From these observations it can be concluded that the twin boundaries occur at irregular intervals. The interval is most commonly either $7a_p$ or $8a_p$, although other intervals occasionally occur.

The large periodicity of the twin boundary spacing in $NaPrMnWO_6$ prohibits us from being able to use the same method to model the satellite peaks in the NPD pattern of this

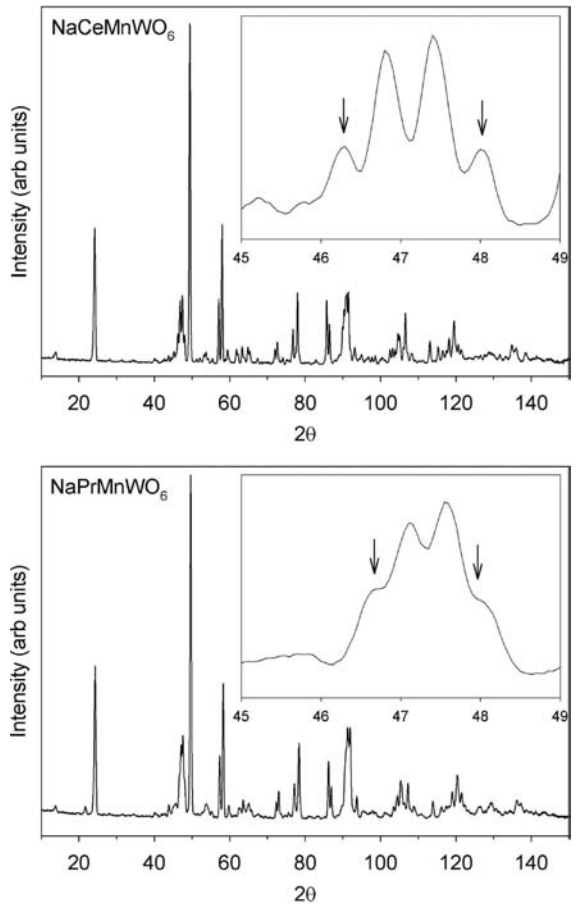

Figure 5. Neutron powder diffraction patterns of $NaCeMnWO_6$ and $NaPrMnWO_6$. The insets show the regions of the patterns where the satellite peaks (marked with arrows) are most pronounced.

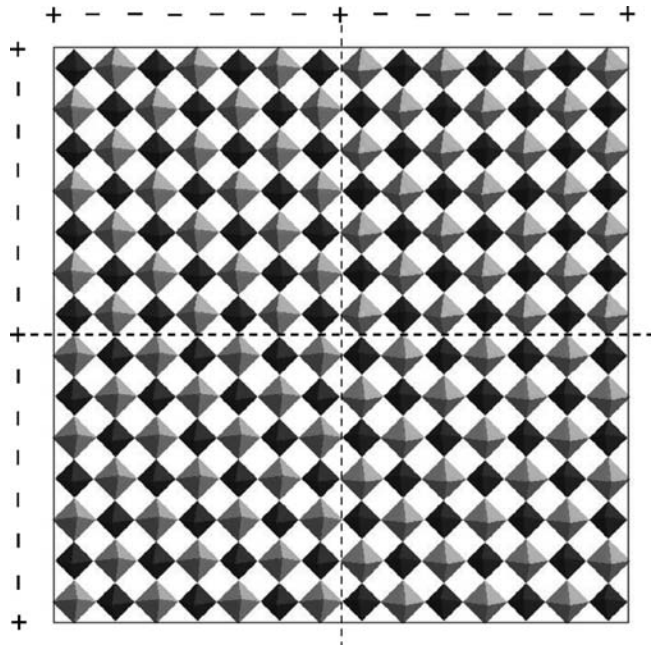

Figure 6. One layer of WO_6 octahedra (black) and MnO_6 octahedra (light gray) in a $14a_p \times 14a_p \times 2a_p$ unit cell. The dotted lines show the locations of the octahedral tilt twin boundaries. The + and − symbols represent in-phase and out-of-phase tilting, respectively.

dx.doi.org/10.1021/ic202071n | Inorg. Chem. 2012, 51, 4007–4014

compound. However, some qualitative observations can still be made. The satellite peaks in $NaPrMnWO_6$ are broader and lie closer to the subcell peaks than in the case of $NaCeMnWO_6$. This implies that the spacing of the twin boundaries is highly irregular, but is on average larger than for $NaCeMnWO_6$. This is consistent with what is observed in the ED and HRTEM patterns.

Synchrotron X-ray Powder Diffraction. Previous analysis of $NaCeMnWO_6$ and $NaPrMnWO_6$ by laboratory XRD suggested a tetragonal $\sqrt{2}a_p \times \sqrt{2}a_p \times 2a_p$ unit cell for both compounds. The high resolution and low background of a synchrotron radiation diffraction pattern should allow us to detect any subtle peak splitting because of lower symmetry as well as any very weak supercell reflections resulting from a superstructure. The synchrotron XRD patterns of both compounds could be adequately modeled by performing a Rietveld refinement using space group *P*4/*nmm*. No splitting of the peaks was evident, confirming that the long-range symmetry is indeed tetragonal. The imperfect fit to some of the peak intensities and unrealistic atomic displacement parameters for several of the atoms is not surprising given the fact that the *P*4/*nmm* model neglects the incommensurate modulation seen by both electron and neutron diffraction. There were a few additional weak peaks evident in the patterns that were not indexed by the *P*4/*nmm* cell. Some of these peaks could be attributed to a small impurity of Na_2WO_4. The presence of this impurity might be associated to existence of a compositional modulation. The Na_2WO_4 impurity was added as a second phase in the refinements, and the molar concentration was refined to be less than 1% in both cases. A second unidentified impurity phase appears to be present in the $NaPrMnWO_6$ sample.

A few other very weak reflections can be attributed to the supercell caused by the octahedral tilt twinning, as they occur at the same *d*-spacings as the strongest satellite reflections in the NPD patterns. These are shown in Figure 7. These peaks are much weaker than in the NPD patterns because of the lower sensitivity of X-rays to oxygen positions. It is worth noting that in our previous work on $KLaMnWO_6$ we were unable to observe any evidence of the superstructure in the synchrotron XRD pattern of this compound, despite the fact that both synchrotron diffraction patterns were collected on ID31 at the ESRF. The reason for this difference could be related to the smaller tolerance factors of $NaCeMnWO_6$ and $NaPrMnWO_6$ compared to $KLaMnWO_6$. The smaller tolerance factors result in larger octahedral tilt angles, which in turn lead to larger atomic displacements and stronger satellite reflections. The satellite peaks in the $NaPrMnWO_6$ pattern are noticeably broader than in $NaCeMnWO_6$ pattern, which is consistent with greater level of irregularity in the superstructure observed by TEM for the Pr compound.

DISCUSSION

The results clearly show that both $NaCeMnWO_6$ and $NaPrMnWO_6$ possess incommensurately modulated crystal structures. Modeling of the neutron diffraction data leaves little doubt that the presence of periodic, but widely spaced in-phase tilts (i.e., octahedral tilt twinning), is at least partially responsible for the modulation.

Among $AA'BB'O_6$ perovskites, $NaCeMnWO_6$ and $NaPrMnWO_6$ are the first compounds known to possess incommensurately modulated structures. The superstructures consist of two types of domains arranged in the form of a chessboard pattern.

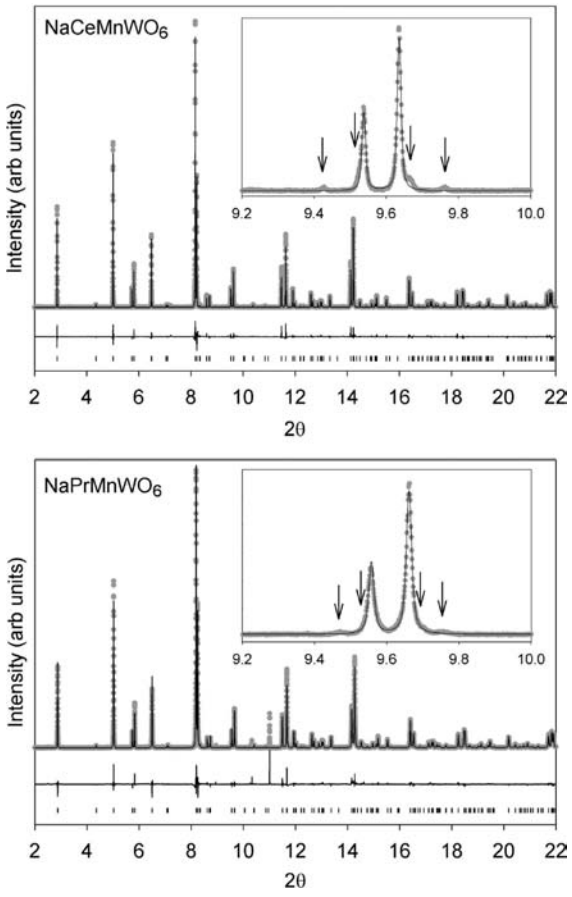

Figure 7. Fits to the synchrotron XRD patterns of $NaCeMnWO_6$ and $NaPrMnWO_6$ using a *P*4/*nmm* model. The insets show the regions of the patterns where the satellite peaks (marked with arrows) are most pronounced. The difference curve is shown beneath, and the tick marks show the positions of the allowed *hkl* reflections.

As shown in Table 1, previous periodicities of $10a_p$, $12a_p$, and $14a_p$ have been observed so far. The average periodicity in

Table 1. Comparison of the Tolerance Factors, the Average Periodicities of the Modulations, Differences in Ionic Radii of the *A* and *A*′ Cations, and the Type of Superlattice That Forms[a] for the $AA'BB'O_6$ Perovskites Whose Superlattices Have Been Studied in Detail

compound	tolerance factor	average periodicity	*A*/*A*′ size difference (Å)	1 or 2-dimensional
$KLaMnWO_6$	0.986	$10a_p$	0.28	2-D
$NaLaMgWO_6$	0.952	$12a_p$	0.03	1-D
$NaNdMgWO_6$	0.940	$14a_p$	0.12	2-D
$NaCeMnWO_6$	0.926	$14.9a_p$	0.05	mostly 2-D/some 1-D
$NaPrMnWO_6$	0.924	$21.7a_p$	0.10	mostly 2-D/some 1-D

[a]2-D chessboard or 1-D stripes.

$NaCeMnWO_6$ is $14.9a_p$ and, the average periodicity in $NaPrMnWO_6$ is about $21.7a_p$. Now that detailed information is available for a number of $AA'BB'O_6$ perovskite superstructures, it is possible to look for trends. One trend that emerges is a correlation between the tolerance factor and the size of the domains. The size of the domains appears to be a function of the tolerance factor, with larger tolerance factors giving rise to smaller domains and smaller tolerance factors

dx.doi.org/10.1021/ic202071n | Inorg. Chem. 2012, 51, 4007–4014

giving rise to larger domains and therefore to larger periodicity (Table 1). Some previous work on lattice parameter trends in the two series Na*Ln*MnWO$_6$ and Na*Ln*MgWO$_6$ has shown that for the smaller tolerance factors monoclinic unit cells result, which implies the disappearance of nanodomain formation. This can be understood in terms of the above-mentioned trend. As the tolerance factor is decreased by substituting smaller *Ln* cations the spacing between the domains grows, until eventually the spacing becomes infinite, or in other words, the modulation vanishes. Once the modulation has vanished, the structure further transitions to the $a^-a^-c^+$ tilting pattern instead of the $a^-a^-c^0$ pattern. The additional tilting is probably needed to stabilize these small tolerance factors. One still puzzling result is why NaLaMnWO$_6$ (with a tolerance factor greater than for the Ce and Pr analogues studied here) does not show structural modulation but instead has a simple $P2_1$ unit cell with $a^-a^-c^+$ tilting. Also, the transition from twinned $a^-a^-c^0$ superstructures to simple $a^-a^-c^+$ unit cells does not occur at the same tolerance factor for both the Na*Ln*MnWO$_6$ and Na*Ln*MgWO$_6$ series. It appears that while the tolerance factor seems to determine the magnitude of the modulation vector, whether or not modulation occurs at all depends on more than just the tolerance factor.

An unanswered question regarding nanodomain formation in *AA′BB′*O$_6$ perovskites is why sometimes 1-D stripes are observed and other times 2-D chessboards formation is observed. Previously, when fewer examples were known, it was suggested that this might be related to the tolerance factor. However, from our current list of examples it is obvious that there is no correlation between the tolerance factor and the preference for stripes or checkerboards. There does appear to be a correlation between the difference in ionic radii of *A* and *A′* and the preference for stripe or chessboard formation. The Na and La cations in NaLaMgWO$_6$ are nearly the same size, and this compound shows a strong preference for stripe formation. In KLaMnWO$_6$ and NaNdMgWO$_6$ the *A*/*A′* size difference is larger and a chessboard pattern is observed in both compounds. The *A*/*A′* size difference in NaCeMnWO$_6$ and NaPrMnWO$_6$ is intermediate. Both these compounds show primarily chessboard formation, with a significant amount stripe formation also present. This suggests the possibility that when *A* and *A′* have similar radii stripes are favored and as the size difference increases chessboards become favored.

Octahedral tilt twinning is also observed in ternary and quaternary systems with perovskite-related structure such as $Th_{1/4}NbO_3$,[20,21] $La_{1/3-x}Li_{3x}NbO_3$,[22] $Nd_{2/3-x}Li_{3x}TiO_3$,[23] and $Na_{0.5}Bi_{0.5}TiO_3$.[24,25] There are two commonalities among these compositions (a) there are two or more *A*-site ions (counting vacancies) and (b) these systems allow for nonstoichiometry within the *A* sublattice. However, superlattice formation is not observed in the $La_{2/3-x}Li_{3x}TiO_3$ system despite having the same characteristics.[26]

CONCLUSIONS

The perovskites NaCeMnWO$_6$ and NaPrMnWO$_6$ both spontaneously form incommensurately modulated crystal structures. The modulated structures consist primarily of two types of domains arranged in the form of a chessboard pattern, although stripe formation is also found in some crystals of each compound. The periodicity in the appearance of the domain boundaries are perturbed by the appearance of domains of different size, which is a deviation from the regular sequence inducing incommensurate positions of the extra reflections in the ED pattern. The average periodicity in NaCeMnWO$_6$ is $14.9a_p$ and in NaPrMnWO$_6$ it is $21.7a_p$. The network of corner sharing MnO$_6$ and WO$_6$ octahedra are tilted according to the $a^-a^-c^0$ system. This pattern of tilts is periodically interrupted by an in-phase tilt. These in-phase tilts, which effectively act as antiphase boundaries with respect to the tilting, are largely responsible for the modulated structure. Features seen in the HRTEM images and comparisons to earlier studies on related compounds suggest that a compositional modulation of the *A*-cation sublattice may also be present. The presence of a compositional modulation of the *A*-site cations could help to explain the presence of antiphase boundaries in the octahedral tilting. By comparison with previously known examples, it appears that the size of the compositional domains is correlated to the tolerance factor, with smaller tolerance factors giving rise to larger domains. It also appears that having a small size mismatch between *A* and *A′* may favor the formation of stripes, while a large size difference favors the formation of 2-D chessboards.

ASSOCIATED CONTENT

Supporting Information

Additional TEM images for NaPrMnWO$_6$. This material is available free of charge via the Internet at http://pubs.acs.org.

AUTHOR INFORMATION

Corresponding Author

*E-mail: gking@lanl.gov.

Notes

The authors declare no competing financial interest.

ACKNOWLEDGMENTS

We thank the Microscopy Centre's Luis Bru from UCM for technical assistance. S.G-M. thanks the Spanish MICINN for funding Project MAT2010-19837-C06-03 and CAM for Project MATERYENER-2, P2009/PPQ-1629. We also thank the Institut Laue-Langevin, Grenoble, France, and the European Synchrotron Radiation Facility, Grenoble, France, for the allocation of beamtime. The authors are grateful to A. Fitch for assistance during the collection of the synchrotron XRD data. P.M.W. would like to recognize financial support from the National Science Foundation (Award number DMR-0907356).

REFERENCES

(1) King, G.; Woodward, P. M. *J. Mater. Chem.* **2010**, *20*, 5785–5796.
(2) Knapp, M. C.; Woodward, P. M. *J. Solid State Chem.* **2006**, *179*, 1076–1085.
(3) King, G.; Thimmaiah, S.; Dwivedi, A.; Woodward, P. M. *Chem. Mater.* **2007**, *19*, 6451–6458.
(4) King, G.; Wayman, L. M.; Woodward, P. M. *J. Solid State Chem.* **2009**, *182*, 1319–1325.
(5) King. G. Ph.D. Dissertation, The Ohio State University, Columbus, OH, 2010.
(6) García-Martín, S.; Urones-Garrote, E.; Knapp, M. C.; King, G.; Woodward, P. M. *J. Am. Chem. Soc.* **2008**, *130*, 15028–15037.
(7) García-Martín, S.; King, G.; Urones-Garrote, E.; Nénert, G.; Woodward, P. M. *Chem. Mater.* **2011**, *23*, 163.
(8) Licurse, M. W.; Davies, P. K. *Appl. Phys. Lett.* **2010**, *97*, 123101.
(9) King, G.; García-Martín, S.; Woodward, P. M. *Acta Crystallogr., Sect. B* **2009**, *65*, 676–683.
(10) Glazer, A. M. *Acta Crystallogr.* **1972**, *B28*, 3384–339.
(11) Glazer, A. M. *Acta Crystallogr.* **1975**, *A31*, 756–76.

(12) Lufaso, M. W.; Woodward, P. M. *Acta Crystallogr., Sect. B* **2001**, *57*, 725−738.
(13) Lufaso, M. W.; Barnes, P. W.; Woodward, P. M. *Acta Crystallogr., Sect. B* **2006**, *62*, 397−410.
(14) Toby, B. H. *J. Appl. Crystallogr.* **2001**, *34*, 210−213.
(15) Larson., A. C.; Von Dreele, R. B. *GSAS: General Structure Analysis System*; Report LAUR 86-748; Los Alamos National Laboratory: Los Alamos, NM, 2004.
(16) Woodward, D. Y.; Reaney, I. M. *Acta Crystallogr., Sect. B* **2005**, *61*, 387−399.
(17) Alario-Franco, M. A.; Grey, I. E.; Joubert, J. C.; Vincent, H.; Labeau, M. *Acta Crystallogr., Sect., A* **1982**, *38*, 177−186.
(18) Labeau, M.; Grey, I. E.; Joubert, J. C.; Vincent, H.; Alario-Franco, M. A . *Acta Crystallogr., Sect. A* **1982**, *38*, 753−761.
(19) García-Martín, S.; Alario-Franco, M. A. *J. Solid State Chem.* **1999**, *148*, 93−99.
(20) van Smaalen, S. *Incommensurate Crystallography*; Oxford University Press Inc.: New York,2007.
(21) Guiton, B. S.; Davies, P. *J. Am. Chem. Soc.* **2008**, *130*, 17168−17173.
(22) Guiton, B. S.; Davies, P. K. *Chem. Mater.* **2008**, *20*, 2860−2862.
(23) Guiton, B. S.; Davies, P. K. *Nat. Mater.* **2007**, *6*, 586−591.
(24) Dorcet, V.; Trolliard, G.; Boullay, P. *Chem. Mater.* **2008**, *20*, 5061−5073.
(25) Dorcet, V.; Trolliard, G.; Boullay, P. *J. Magn. Magn. Mater.* **2009**, *321*, 1762−1766.
(26) García-Martín, S.; Alario-Franco, M. A.; Ehrenberg, H.; Rodríguez-Carvajal, J.; Amador, U. *J. Am. Chem. Soc.* **2004**, *126*, 3587−3596.

NOTE ADDED AFTER ASAP PUBLICATION

Due to a production error, this paper was published on the Web on March 2, 2012, with minor text errors. The corrected version was reposted on March 12, 2012.